Materials Research Proceedings 28 (2023) 101-110 https://doi.org/10.21741/9781644902479-12

In process monitoring of geometrical characteristics in laser metal deposition: A comparative study

LATTE Marco[1,a *], GUERRA Maria Grazia[1,b], MAZZARISI Marco[1,c], ANGELASTRO Andrea[1,d], CAMPANELLI Sabina Luisa[1,e] and GALANTUCCI Luigi Maria [1,f]

[1]Dept. of Mechanics, Mathematics and Management, Politecnico di Bari, Via Orabona 4 - 70125 Bari, Italy

[a]marco.latte@poliba.it, [b]mariagrazia.guerra@poliba.it, [c]marco.mazzarisi@poliba.it, [d]andrea.angelastro@poliba.it [e]sabinaluisa.campanelli@poliba.it, [f]luigimaria.galantucci@poliba.it

Keywords: Laser Metal Deposition, Process Monitoring, Image Processing, Laser Line

Abstract. Although it is experiencing a wide diffusion, there are still several limits to the use of additive manufacturing (AM) for the fabrication of metal components. This includes low productivity, poor dimensional accuracy and uncertainty about the mechanical properties of the final parts. The main cause of these undesirable effects lies in the intrinsic complexity of the metal AM processes, such as Laser Metal Deposition (LMD). Accurate monitoring of the process and optimization of the process parameters are therefore of fundamental importance to ensure the overall quality of the product. Nowadays, several optical methods are under development for the monitoring of geometric characteristics and their correlation with specific process parameters, such as the standoff distance. This paper presents a comparative study between two optical in-process monitoring methods performed on AISI 316L multilayer samples produced by the LMD process. The first is a laser line section method based on a laser diode mounted on the deposition head, while the second method uses a high-resolution CMOS camera placed on the horizontal plane with a front view of the sample. In both cases, ad-hoc image processing algorithms were used to process the data, reconstruct the morphology of the component, and extract geometrical information. Results were then validated using an offline scanning system and micrographic analyses. Both proposed systems allowed the monitoring of the deposition quality using appropriate Key Performance Indicators (KPIs). The study showed a good capability of the prototype systems to detect deposition defects due to undesired variations of the process conditions and to monitor the standoff distance.

Introduction

Despite the widespread adoption of additive manufacturing (AM), there are still several limitations to the use of some technologies for the fabrication of metal components. Laser Metal Deposition (LMD) is an AM technique implemented in several industrial sectors thanks to its several advantages. Although it is still characterized by poor dimensional accuracy, mainly due to variable thermal cycling, localized heat accumulation, irregular powder flow, etc. [1]. In-situ monitoring and process control can be used for avoiding unpredictable build failures and minimizing the time and cost of post-process characterization procedures [2].

The monitoring of the LMD process is carried out in different fields: monitoring of the thermal field for the high temperatures developed by the laser during the process [3], monitoring of the powder flow [4] and monitoring of geometrical parameters of the produced component [5]. Among the several outputs that need to be monitored and controlled to ensure the quality of the process/component, standoff distance and layer height are very important. In fact, a wrong standoff distance can lead to height deviations from the ideal building path [6].

Nowadays, several optical methods are under development for the monitoring of geometric characteristics and their correlation with specific process parameters. These methods are based mainly on the use of CCD/CMOS camera, laser scanners and structured light scanners.

The CCD/CMOS cameras are widely used, as they are flexible and easy to implement. These systems can be used to monitor the melt pool geometry, its temperature, and the layer height during the process. Although, these method are not particularly suited for the evaluation of complex freeform geometries and they have been mostly applied to simple geometries such as thin walls [7]. In some monitoring system setups, the CCD/CMOS cameras are mounted on the deposition head. Toyserkani and Khajepour [8] studied a closed-loop control system for LMD process, based on a CCD or CMOS camera. A pattern recognition algorithm returned the tracks height and the angle of solid/liquid interface in real-time and the PID controller used these feedbacks to modify the laser pulse energy in order to improve the output. Hsu et al. [9] proposed a vision-based inspection system made up of three digital cameras for measuring the cladding height in the Direct Energy Deposition (DED) process. After the calibration of the system, an image-processing technique is employed to isolate the laser nozzle and the melt pool in the captured images. The height of the coating is then calculated using the distance between the nozzle tip and the center of the melt pool.

On the other hand, laser scan systems are also implemented in various works in the literature. This technique is based on the triangulation principle and, mounting the equipment on the deposition head, a three-dimensional representation of the built component can be obtained [10]. With respect to the CCD/CMOS cameras, this monitoring technique is usually more expensive and require additional movements of the deposition head during scanning. Nevertheless, the monitoring of complex geometries is less difficult to perform. In [11], Rodriguez-Araujo et al. used a scanning system based on a CMOS camera coupled to a laser line mounted to the laser head to acquire the 2D profiles of the deposited layers. Cao et al. [12] used a commercial laser displacement sensor to study the surface topography detection of 24CrNiMo alloy steel produced by direct laser deposition. Arejita et al. [13] presented a closed-loop control algorithm that dynamically controlled the melt pool size, deposition speed and standoff distance combining data from a laser line profiler and a NIT Tachyon 1024 micro-core MWIR camera.

Structured light 3D imaging systems project coded patterns into the object rather than a single line and utilize a coding approach to calculate the depth of each observed point. The precision of the measurements strongly depends on the calibration of the equipment according to the measured volume, but an acceptable accuracy can also be obtained by basic equipment [7]. Some authors have used a 3D scanner to monitor the part geometry [14]. Garmendia et al. [15] have integrated a structured light-based scanner into a DED system in order to obtain a complete reconstruction of the manufactured geometry, making possible to monitor the product quality while it is being built, avoiding any suspension of the production process or offline measurement.

Due to the high cost of the components, the complexity of the additional movements required for 3D scanning and the harsh environment in which the systems are operating, laser line scanners and structured light 3D imaging have become popular only in recent years [7].

Regarding the investigated geometries, in the literature, most studies deal with the monitoring of monolayers or thin walls component [16,17], while few studies focus on the geometric monitoring of massive and multilayer components made by LMD [18,19].

This work presents a comparative study between two optical in-process monitoring methods performed on AISI 316L massive multilayer samples produced by the LMD process. The first is a laser line section method (LL) based on a laser diode mounted on the deposition head, while the second method uses a high-resolution CMOS camera (FC from now on) placed on the horizontal plane with a front view of the sample. In both cases, ad-hoc image processing algorithms were used to process the data, reconstruct the morphology of the component, and extract geometrical

information. Results were then validated through an offline scanning system and micrographic analyses.

Material and Methods

The monitoring systems compared in this work were a laser line scanner and a high-resolution camera (Fig. 1(a)). The first system comprised a laser line diode with λ=532 nm and 5 mW of power as light source and an industrial CMOS camera (IDS UI148xSE-C) as receiver equipped with a 12.5 mm lens. These two components were assembled on an aluminum support structure properly designed to make the system configuration flexible according to the sample geometry. This system was configured as a layer wise system and it requires an additional movement of the deposition head after the completion of each layer. Data were acquired in a video format with a framerate of 8 frame/sec, while the scan speed was set to 200 mm/min (equal to the deposition speed). In this way the resolution, meant as the distance between two adjacent points on each single profile, was on the order of 0.06 mm, while the resolution along the scan axis was on the order of 0.4 mm depending on the camera frame rate and scan speed.

The second monitoring system consisted of a high-resolution camera, DSLR CANON EOS 760D equipped with a 50 mm lens focused on its minimum distance. The camera was placed on the horizontal plane with the lens oriented to get the sample length (Fig. 1(a)).

With the aim to compare the above-described systems, two samples (sample A and B in Fig. 1(b)) were fabricated by means of a LMD system, with the same material, geometry, and process parameters.

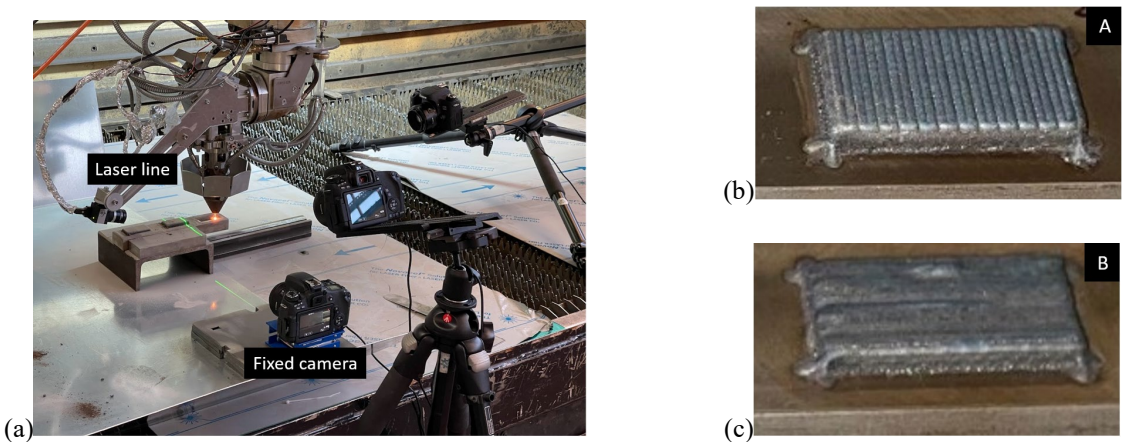

Fig. 1. (a) LMD with the monitoring systems (laser line on the left and fixed camera on the bottom), (b) sample A and (c) sample B.

The LMD system was a prototypal machine composed of a 3 kW CO_2 laser source and a pneumatic powder supply system. The AISI 316L stainless steel powders were carried by the gas to the 3-way multijet nozzle that conveyed them into the melt pool. Helium with a flow rate of 5 lpm was used as carrier gas, while with a flow rate of 11 lpm was used as shielding gas. The spot diameter was equal to 2 mm. The substrates (with a thickness of 25 mm) were also made of AISI 316L stainless steel. The samples were multilayer massive blocks (10 layers) with dimensions of 25 x 50 mm^2. These components were realized by adopting a bidirectional hatch strategy with a 90° rotation of the deposition direction at each layer and consequent modification of the deposition starting point. A 30% overlap between adjacent tracks was used. The sample A was realized in standard operating conditions, while during the fabrication of the sample B, defects were induced: laser shutdown at layer 3, powder flow suspension at layer 5, and deposition speed variations (50% and 150%) at layer 7.

Materials Research Proceedings 28 (2023) 101-110 https://doi.org/10.21741/9781644902479-12

Both methods followed a similar workflow, as shown in Fig. 2. The laser line scanner (LL), after the frame extraction and image processing (conducted by using an ad-hoc MATLAB algorithm), provided a detailed 3D point cloud of each sample layer. The latter was analyzed by GOM Inspect software for the computation of specific process indexes in order to check their suitability for process anomalies and defect detection. On the other hand, after the frame extraction and image processing, the high-resolution fixed camera (FC) provided a 2D single profile of the sample which was a local description of the geometry of the sample (the track facing the camera).

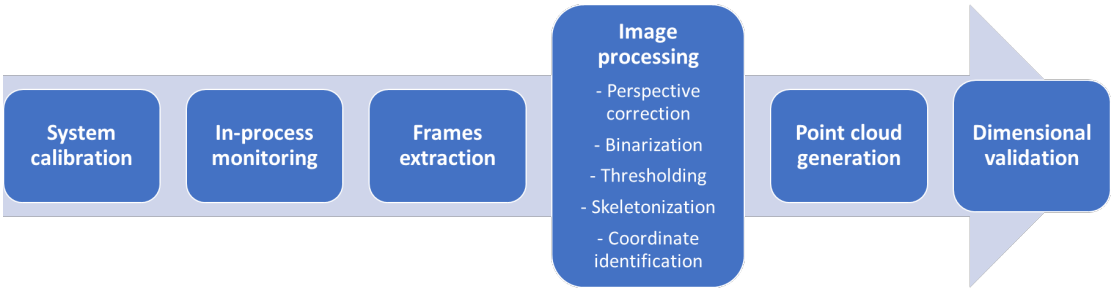

Fig. 2. Process monitoring workflow.

The collected data from both monitoring systems were then analyzed considering geometrical parameters. The average layer height was evaluated as the average distance of each layer point with respect to the base plate. The min-max layer height range and standard deviation were also considered.

The actual standoff distance was calculated as the difference between the design height of the tool center point (i.e., the tip of the nozzle) with respect to the base plate and the average height of the deposited layers, measured with the monitoring methods described above. In this way, it was evaluated the actual distance of the nozzle from the deposition plane and it was compared with the design (theoretical) standoff distance (*SOD_T*), which was set at 12 mm for this kind of nozzle. As can be seen from Fig. 3(a), the FC analysis of the different parameters can be done in-process. On the contrary, the LL analysis is performed at the end of the deposition of each layer. Fig. 3(b) shows one of the frames processed with this last method.

(a) 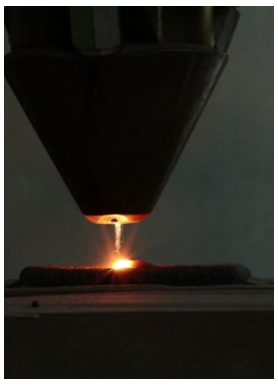 (b) 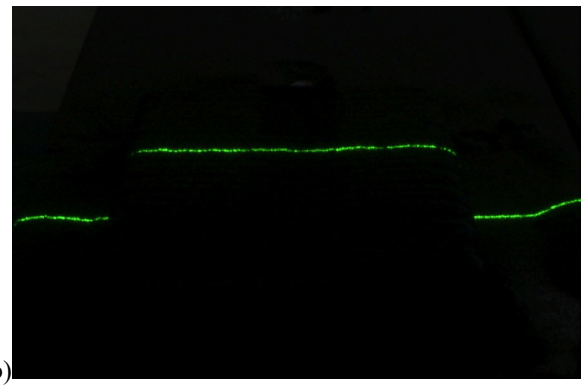

Fig. 3. (a) Frame analyzed by the FC system and (b) by LL system.

The validation procedure of the considered monitoring methods was carried out with an offline 3D scanning system (HandySCAN 3D by Creaform) with known accuracy used for the reconstruction and measurement of the external surface of the entire samples. Additionally, the samples were trimmed, polished and chemically etched, in order to perform a micrographic analysis (Hirox MXB-10C) for estimating the height value of each deposited layer.

Results and Discussion

The point clouds collected for each layer by the LL system were analyzed by means of the GOM Inspect software and, as first check, a colored map was extracted showing the height of each point with respect to the base plate (see Fig. 4). As it is possible to observe, the colored maps well described the layer surface, highlighting the differences between sample A and B with the detection of the areas affected by the induced defects. More in details, at layer 3 the laser shutdown produced a lack in the deposited material, which can be seen from the missing traces on the layer surface. At layer 5, the interruption of the powder flow had a similar effect on the part morphology. It is worth highlighting also how at layer 5 there is still a propagation of the defect induced at layer 3. Finally, at layer 7 the variation of the deposition speed induced a huge protrusion. It was not possible to perform the same analysis by the high-resolution camera due to the different nature of the two monitoring systems.

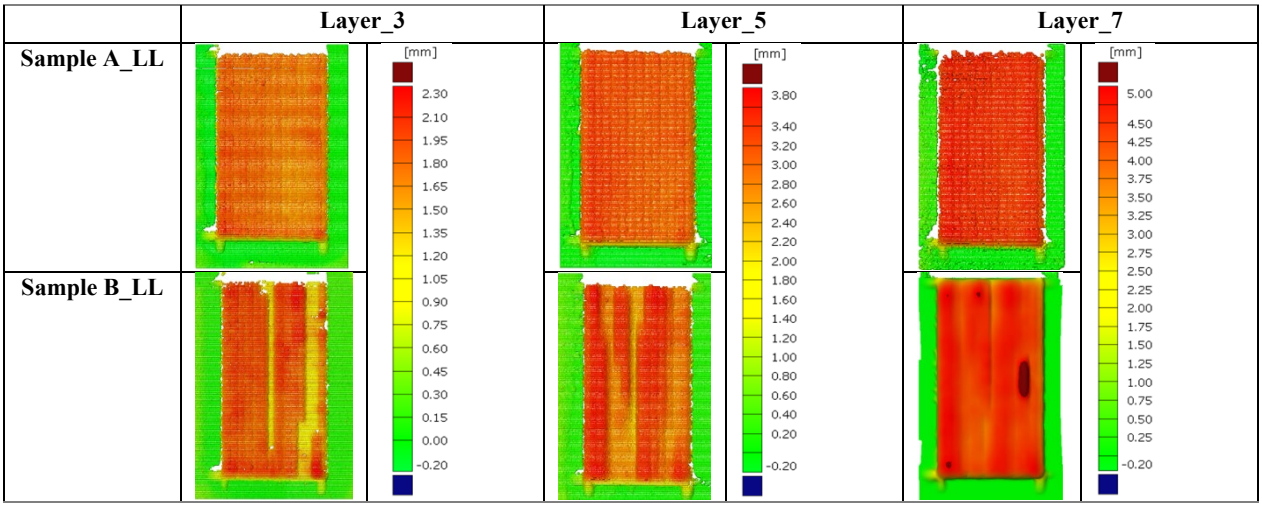

Fig. 4. Colored map showing the layer surface at layer 3, 5 and 7.

After the analysis of the entire layer surface made on the LL point clouds, the cumulative average height and the average layer height for each layer were evaluated for both LL and FC systems. The min-max height range and standard deviation were also computed in order to examine the variability within the entire layer surface for the LL and along the single profile for the FC. As shown in the Fig. 5(a), referring to the sample A, both systems enabled the effective monitoring of the cumulative average height (*H_avg*), showing a quite good convergence. This is because the layer surface was fairly homogeneous, without significant irregularities and defects, in accordance with the micrographic data and scan performed by the HandySCAN 3D. As reported in Fig. 5(b), the layer height values evaluated for each deposited layer (*Delta_H*) were quite similar with maximum differences on the order of 0.15 mm. It was also noted that the standoff distance (*SOD*) tends to decrease with the increase of the layer number. Slight reductions in standoff distance usually leads to a variation in the laser power density and powder flow distribution, deviating from the optimal conditions [4]. As a result, the amount of caught powder and the layer height decreases [20].

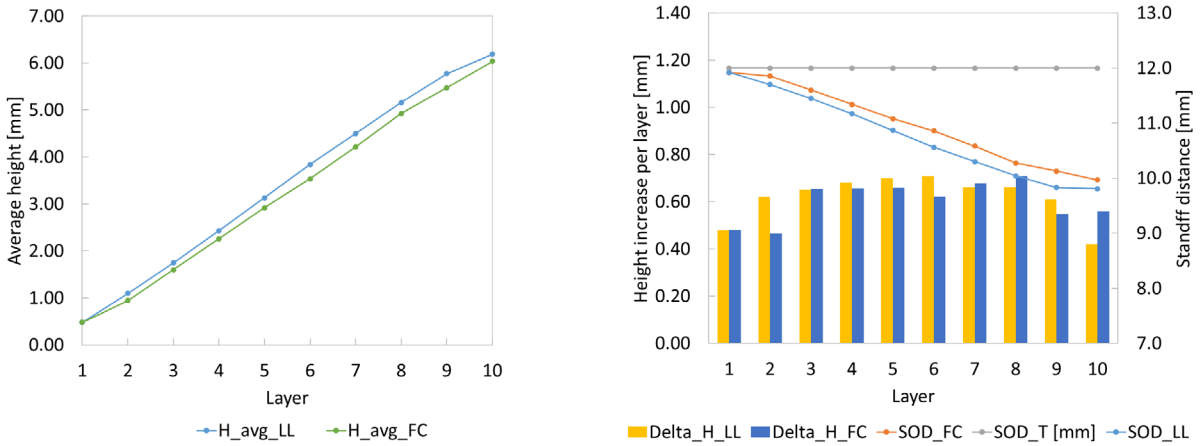

(a) (b)

Fig. 5. (a) Cumulative average height and (b) average layer height evaluated for each layer of the sample A.

The same evaluations were carried out on sample B. In this case, as can be observed from the graph (see Fig. 6), the deposition of ten layers was not possible as for sample A, due to the critical reduction of the standoff distance at layer 7 (layer growth higher than expected). The abrupt standoff distance reduction is to be avoided because it can cause equipment problems due to close interaction between nozzle and component. Considering the cumulative average height (see Fig. 6(a)) and the layer height (see Fig. 6(b)), there was still a convergence of results, with a significant difference registered at layer 5 where, from the colored map reported in Fig. 4, defects due to the powder flow interruption and the propagation of defect induced at layer 3 can be observed.

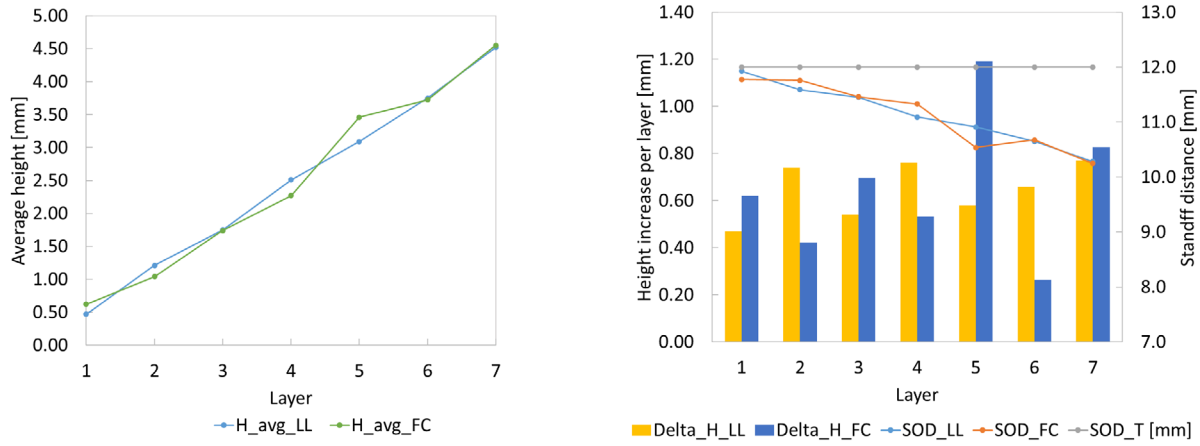

(a) (b)

Fig. 6. (a) Cumulative average height and (b) average layer height evaluated for each layer of sample B.

More generally, due to the 2D nature of the data coming from the FC, only the upper profile of the part facing the camera can be evaluated. This means that every process anomaly causing lack of materials within the layer, not affecting the first trace, is undetectable by this monitoring system (layer 5). On the other hand, when defects cause protrusions (anomalous material accumulation) within the deposited layer, even if these are not located along the side facing the camera, the FC technique is capable of detecting the irregularity (layer 7). Considering the layer 3, quite a good

convergence was found between LL and FC even in the presence of lack of material due to the laser interruption. Although, the area affected by the defect has a small extension with respect to the entire layer surface (see the colored map in Fig. 4), and it had a little influence on the average height value.

The standoff distance was also almost convergent with a more significant deviation registered at layer 5, for the above-mentioned reasons. Thus, both systems enabled the effective monitoring of the individual layer height and cumulative average height of the component, as well as the evaluation of the standoff distance for sample A and, to some extent, also in the presence of induced defects (sample B).

Although, from a monitoring point of view, the average layer height did not clearly indicate the onset of defects observed on sample B. For this reason, besides the average value, the min-max layer height range (*Range*) and standard deviation (*Std_Dev*) were also considered for the defect detection. In this case, considering first the LL system, there was an increase of these two indicators at layer 3, propagating at layer 4, a subsequent increase at layer 5 and another increase at layer 7 in correspondence of the last induced defect (see Fig. 7(a)).

Considering the FC system (Fig. 7(b)), in this case the range and the standard deviation were less sensitive to the induced defects except for the layer 7. The FC system indeed is capable of identifying, apart from the track facing the camera, only protrusions and accumulation of material exceeding the height of the visible track, see Fig. 3(a). Defects in the form of lack of material are not identified by this method.

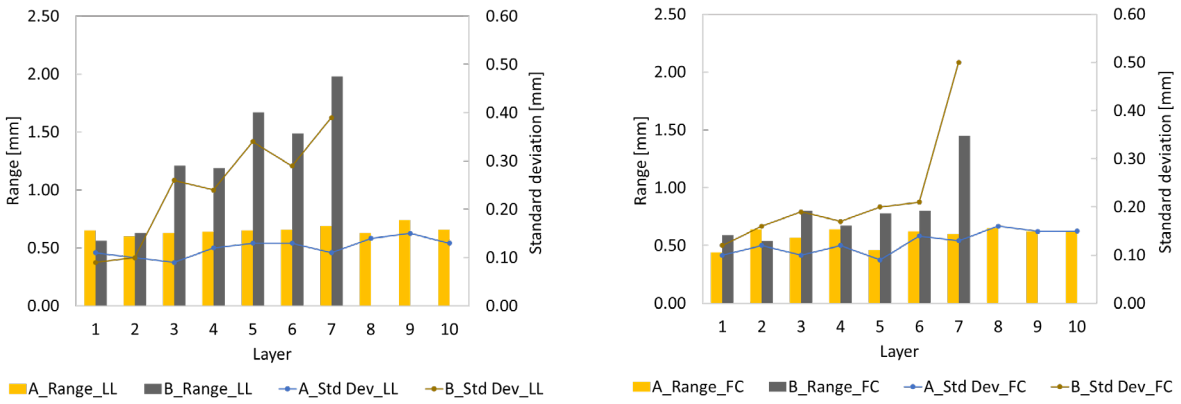

(a) (b)

Fig. 7. (a) Monitoring of the min-max layer height range and standard deviation performed by the LL method and (b) performed by the FC method.

Finally, the validation of the monitoring results was carried out considering the 3D reconstruction and the micrographic analysis of sample A. In the first method, the validation was conducted on the sample A. With this aim, a 3D comparison between the point cloud of the layer 10 obtained with the LL and the mesh obtained with the HandySCAN arm was carried out (see Fig. 8(a)). The estimated absolute average deviation was on the order of 0.055 mm, with maximum values approaching 0.2 mm. These deviations could be caused by unmolten residual powder that remains on the sample after the last layer deposition and which the process gas is unable to move away from the sample. This thin film of powder could slightly alter the in process scanning with LL.

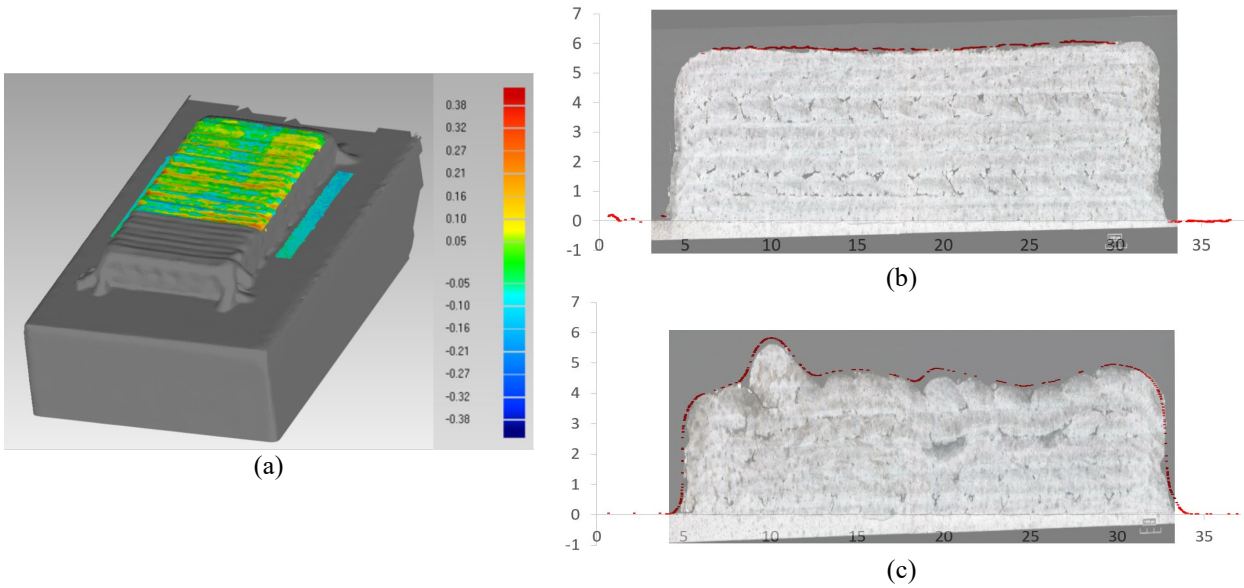

Fig. 8. (a) Comparison between the point cloud of the layer 10 obtained by the LL technique and the mesh obtained by the HandySCAN arm for sample A; (b) comparison between macrography and profile obtained by the LL method for sample A and (c) sample B.

The second method for the validation was a micrographic analysis. From Fig. 8(b) it is possible to observe a good correspondence between the transversal profile extracted from the LL system and the cross-section achieved by the micrographic analysis. Using this method, it was possible to evaluate the cumulative average height as well as each average layer height on the sample section. Micrographic analysis of sample B was also performed and compared with the profile extracted from a corresponding section (Fig. 8(c)).

Results for sample A are then reported in Fig. 9. The maximum deviation found with respect to metallography, for both techniques, was 0.13 mm.

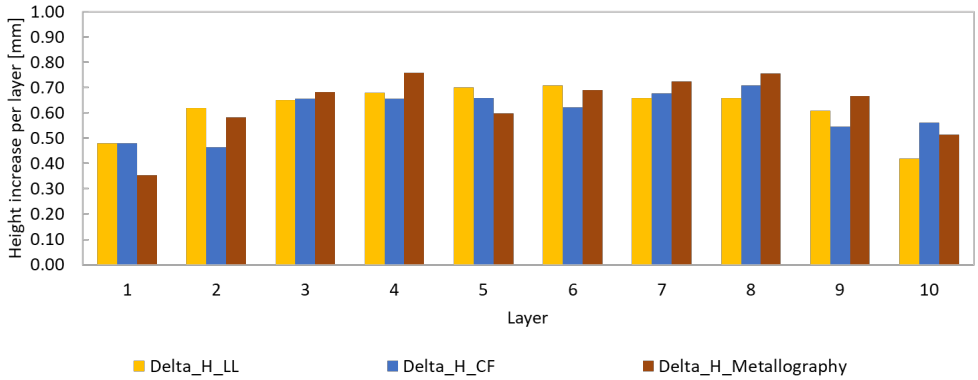

Fig. 9. Comparison of layers average heights as determined using each of the methods.

Summary

A comparative study between two optical in-process monitoring methods performed on AISI 316L multilayer samples produced by the LMD process has been presented. The first was a laser line section (LL) method based on a laser diode mounted on the deposition head, while the second method used a high-resolution CMOS camera placed on the horizontal plane (FC) with a front view of the sample. The systems enabled the effective monitoring of the average height of deposited layers and of the standoff distance. These also allowed the monitoring of the deposition

quality by means of appropriate KPIs as the min-max layer height range and standard deviation. The conducted analysis has shown remarkable results:

- The LL system was capable of evaluating the entire layer surface. At first, the 3D comparison tool allowed the detection of all the induced process defects in both forms, lack of material (layer 3 and 5) and material accumulation (layer 7). It was also possible to assess the average layer height, the min-max range and the standard deviation of the height values recorded at each layer, allowing a rapid detection of process defects.
- The FC system was capable to retrieve a single profile of the side facing the camera, which was almost sufficient to describe the layer geometry for the sample A (without induced defects), but it became ineffective when tested on sample B for the detection of defects in the form of lack of material.
- Regarding the standoff distance evaluation, the FC method offer the possibility to measure it directly via image analysis (nozzle – part distance), while the LL method allows only an indirect computation through the calculation of the height of the part.
- Both methods are threshold dependent in the image analysis, especially the FC when it is used in-process due to continuous variation of environmental light conditions. The use of illuminators is than recommended, in both closed and open chamber applications.
- Another important criterion for comparing the LL and FC methods is the capability to work in-process. In this case the FC method has advantages because it can work in-process and it does not require an additional movement of the deposition head to measure the layer surface. In this way, it can evaluate both the layer height and the standoff distance and it can generate an alert when the measured values exceed selected safety thresholds. On the other hand, the FC method appears to be more suitable for single track monitoring and generally simple geometries, while LL is more suitable for complex geometries requiring multi track and multilayer strategies.

Acknowledgements
This research work was undertaken in the context of the project PON ―R&I 2014 - 2020 ARS01_00906 ―Soluzioni Innovative per la qualità e la sostenibilità dei processi di ADDitive manufacturing.

References
[1] F. Kaji, H. Nguyen-Huu, A. Budhwani, J.A. Narayanan, M. Zimny, E. Toyserkani, A deep-learning-based in-situ surface anomaly detection methodology for laser directed energy deposition via powder feeding, J. Manuf. Process. 81 (2022) 624-637. https://doi.org/10.1016/j.jmapro.2022.06.046
[2] L. Yi, A. Shokrani, R. Bertolini, U. Mutilba, M.G. Guerra, E.G. Loukaides, P. Woizeschke, Optical sensor-based process monitoring in additive manufacturing, Procedia CIRP 115 (2022) 107-112. https://doi.org/10.1016/j.procir.2022.10.058
[3] M. Mazzarisi, A. Angelastro, M. Latte, T. Colucci, F. Palano, S.L. Campanelli, Thermal monitoring of laser metal deposition strategies using infrared thermography, J. Manuf. Process. 85 (2023) 594-611. https://doi.org/10.1016/j.jmapro.2022.11.067
[4] M. Mazzarisi, V. Errico, A. Angelastro, S.L. Campanelli, Influence of standoff distance and laser defocusing distance on direct laser metal deposition of a nickel-based superalloy, Int. J. Adv. Manuf. Technol. 120 (2022) 2407-2428. https://doi.org/10.1007/s00170-022-08945-3
[5] M.G. Guerra, V. Errico, A. Fusco, F. Lavecchia, S.L. Campanelli, L.M. Galantucci, High resolution-optical tomography for in-process layerwise monitoring of a laser-powder bed fusion technology, Additive Manufacturing 55 (2022) 102850. https://doi.org/10.1016/j.addma.2022.102850

[6] H. Borovkov, A.G. de la Yedra, X. Zurutuza, X. Angulo, P. Alvarez, J.C. Pereira, F. Cortes, In-Line Height Measurement Technique for Directed Energy Deposition Processes, JMMP 5 (2021) 85. https://doi.org/10.3390/jmmp5030085
[7] I. Garmendia, J. Leunda, J. Pujana, A. Lamikiz, In-process height control during laser metal deposition based on structured light 3D scanning, Procedia CIRP 68 (2018) 375-380. https://doi.org/10.1016/j.procir.2017.12.098
[8] E. Toyserkani, A. Khajepour, A mechatronics approach to laser powder deposition process, Mechatronics. 16 (2006) 631–641. https://doi.org/10.1016/j.mechatronics.2006.05.002.
[9] H.-W. Hsu, Y.-L. Lo, M.-H. Lee, Vision-based inspection system for cladding height measurement in Direct Energy Deposition (DED), Additive Manufacturing 27 (2019) 372-378. https://doi.org/10.1016/j.addma.2019.03.017
[10] S. Donadello, M. Motta, A.G. Demir, B. Previtali, Coaxial laser triangulation for height monitoring in laser metal deposition, Procedia CIRP 74 (2018) 144-148. https://doi.org/10.1016/j.procir.2018.08.066
[11] J. Rodriguez-Araujo, J.J. Rodriguez-Andina, ROS-based 3D on-line monitoring of LMD robotized cells, in: 2015 IEEE 13th International Conference on Industrial Informatics (INDIN), IEEE, Cambridge, United Kingdom, 2015, pp. 308–313. https://doi.org/10.1109/INDIN.2015.7281752
[12] L. Cao, S. Chen, M. Wei, Q. Guo, J. Liang, C. Liu, M. Wang, Study of surface topography detection and analysis methods of direct laser deposition 24CrNiMo alloy steel, Optics & Laser Technology 135 (2021) 106661. https://doi.org/10.1016/j.optlastec.2020.106661
[13] B. Arejita, I. Garmendia, J.F. Isaza, A. Zuloaga, Dynamic control for LMD processes using sensor fusion and edge computing, Procedia CIRP 111 (2022) 308-312. https://doi.org/10.1016/j.procir.2022.08.026
[14] I. Garmendia, J. Pujana, A. Lamikiz, J. Flores, M. Madarieta, Development of an Intra-Layer Adaptive Toolpath Generation Control Procedure in the Laser Metal Wire Deposition Process, Materials 12 (2019) 352. https://doi.org/10.3390/ma12030352
[15] I. Garmendia, J. Flores, M. Madarieta, A. Lamikiz, L.G. Uriarte, C. Soriano, Geometrical control of DED processes based on 3D scanning applied to the manufacture of complex parts, Procedia CIRP 94 (2020) 425–429. https://doi.org/10.1016/j.procir.2020.09.158
[16] M. Borish, B.K. Post, A. Roschli, P.C. Chesser, L.J. Love, K.T. Gaul, Defect Identification and Mitigation Via Visual Inspection in Large-Scale Additive Manufacturing, JOM 71 (2019) 893-899. https://doi.org/10.1007/s11837-018-3220-6
[17] J. Ye, N. Alam, A. Vargas-Uscategui, M. Patel, A. Bab-Hadiashar, R. Hoseinnezhad, I. Cole, In situ monitoring of build height during powder-based laser metal deposition, Int. J. Adv. Manuf. Technol. 122 (2022) 3739-3750. https://doi.org/10.1007/s00170-022-10145-y
[18] P. Xu, X. Yao, L. Chen, C. Zhao, K. Liu, S.K. Moon, G. Bi, In-process adaptive dimension correction strategy for laser aided additive manufacturing using laser line scanning, J. Mater. Process. Technol. 303 (2022) 117544. https://doi.org/10.1016/j.jmatprotec.2022.117544
[19] I. Garmendia, J. Pujana, A. Lamikiz, M. Madarieta, J. Leunda, Structured light-based height control for laser metal deposition, J. Manuf. Process. 42 (2019) 20-27. https://doi.org/10.1016/j.jmapro.2019.04.018
[20] H. Tan, W. Shang, F. Zhang, A.T. Clare, X. Lin, J. Chen, W. Huang, Process mechanisms based on powder flow spatial distribution in direct metal deposition, J. Mater. Process. Technol. 254 (2018) 361–372. https://doi.org/10.1016/j.jmatprotec.2017.11.026